Int. J. Heat Mass Transfer. Vol. 33, No. 6, pp. 1047–1055, 1990
Printed in Great Britain

0017–9310/90 $3.00 + 0.00
Pergamon Press plc

Turbulent gas flow heat transfer and friction in channels of different cross-sections

A. I. LEONTIEV, B. B. PETRIKEVICH and O. G. VYRODOV
N. E. Bauman Higher Technical College, Moscow, 107005, U.S.S.R.

(*Received* 5 *April* 1988)

Abstract—Consideration is given to gas flow in channels of circular, annular and plane cross-sections. A mathematical model is suggested which uses an integral approach for describing momentum and energy transfer in a turbulent boundary layer. It is assumed that dynamic and thermal boundary layers start to develop on the channel walls simultaneously and subsequently converge.

1. INTRODUCTION

FOR THE most part, the heat transfer sections of power plants are fabricated in the form of channels of different cross-sections. In general, the mode of gas flow in such channels is turbulent. In such cases, the friction and heat transfer coefficients are traditionally calculated along two lines—experimentally and theoretically. In engineering calculations, the available dimensionless relations for complex unsteady-state boundary conditions [1, 2] are widely applied, especially when the case of interest coincides with the conditions for which some experimental relation was obtained. It should be kept in mind, however, that dimensionless relations obtained for analogous conditions of flow, but by different authors, may differ.

As regards the range of the results being obtained, the theoretical approach is more attractive. However, numerical solution of turbulent boundary layer heat transfer equations in Navier–Stokes' or Prandtl's forms requires unjustifiably great machine time expenditures in many practically important cases. Moreover, the employment of a considerable number of empirical constants to find correlations between turbulence characteristics restricts the potentialities of this approach.

At the present time, for solving a wide class of heat transfer problems, the prediction methods are being developed and applied which realize the integral momentum, heat and mass conservation equations in Karman's form. While retaining the appropriate accuracy, the integral methods require less machine time. Based on the integral method suggested in ref. [3], the present paper investigates the problem of friction and heat transfer of a turbulent gas flow in channels of circular, annular and plane cross-sections. In the general case, heat transfer in annular and plane channels can be asymmetric. It is assumed that thermal and dynamic boundary layers start to develop simultaneously from the channel inlet on both channel walls and that they subsequently converge.

2. MATHEMATICAL MODEL

The equations of heat transfer and friction in a turbulent boundary layer in Prandtl's form are formulated as follows:

$$\frac{\partial \rho}{\partial t}+\frac{1}{H_3^\gamma}\left[\frac{\partial}{\partial x}(\rho V_x H_3^\gamma)+\frac{\partial}{\partial y}(\rho V_y H_3^\gamma)\right]=0 \quad (1)$$

$$\rho\frac{\partial V_x}{\partial t}+\rho V_x\frac{\partial V_x}{\partial x}+\rho V_y\frac{\partial V_x}{\partial y}=-\frac{\partial P}{\partial x}+\frac{1}{H_3^\gamma}\frac{\partial}{\partial y}(H_3^\gamma\tau) \quad (2)$$

$$\rho\frac{\partial h^*}{\partial t}+\rho V_x\frac{\partial h^*}{\partial x}+\rho V_y\frac{\partial h^*}{\partial y}=\frac{\partial P}{\partial t}-\frac{1}{H_3^\gamma}\frac{\partial}{\partial y}(H_3^\gamma q). \quad (3)$$

The boundary conditions are

$$t=0:\quad V_{x01}=V_{\text{in}};\quad h_{\text{w}}^*=h_{\text{in}}^*;\quad P_{01}=P_{\text{in}};$$

$$y=0:\quad -\frac{\lambda}{C_p}\frac{\partial h^*}{\partial y}=q_{\text{w1}};\quad h^*=h_{\text{w1}};$$

$$\rho V_y=(\rho V_y)_{\text{w2}};\quad V_x=0;$$

$$y=S:\quad -\frac{\lambda}{C_p}\frac{\partial h^*}{\partial y}=q_{\text{w2}};\quad h^*=h_{\text{w2}};$$

$$\rho V_y=(\rho V_y)_{\text{w2}};\quad V_x=0; \quad (4)$$

$\gamma=1$ in the annular channel, $\gamma=0$ in the plane channel.

For the initial section of the channel in the region of inviscid flow, $\delta_1\leqslant y\leqslant S-\delta_2$, equations (2) and (3) yield

$$\rho_{\text{e}}\frac{\partial V_{x\text{e}}}{\partial t}+\rho_{\text{e}}V_{x\text{e}}\frac{\partial V_{x\text{e}}}{\partial x}=-\frac{\partial P}{\partial x} \quad (5)$$

$$\rho_{\text{e}}\frac{\partial h_{\text{e}}^*}{\partial t}+\rho_{\text{e}}V_{x\text{e}}\frac{\partial h_{\text{e}}^*}{\partial x}=\frac{\partial P}{\partial t}. \quad (6)$$

Density is defined by the state equation

NOMENCLATURE

b_w permeability parameter of permittivity, $(\rho V_y)_w/\rho_e V_e$
C_p specific heat at constant pressure
C_f friction factor, $2\tau_w/\rho_e V_e^2$
C_v specific heat at constant volume
H form parameter, δ^*/δ^{**}
H' form parameter, $\delta^{*'}/\delta^{**}$
H'_h form parameter, $\delta_h^{*'}/\delta_h^{**}$
H_3 Lamé coefficient, $R_w \pm y\cos\beta$
h total thermodynamic enthalpy
h_r^* recovery enthalpy, $h + r(V_x^2/2)$
h^* stagnation enthalpy, $h + V_x^2/2$
Δh_1 difference of enthalpies, $h_{re}^* - h_w$
Δh difference of enthalpies, $h_e^* - h_w$
I_1 $\int_0^{\delta_1} H_3^\gamma \, dy$
I_2 $\int_0^{\delta_2} H_3^\gamma \, dy$
I_3 $\int_0^{s} H_3^\gamma \, dy$
K ratio of specific heats, C_p/C_v
L characteristic dimension
P pressure
Pr Prandtl number
q heat flux density
R radius
r recovery coefficient
Re_L Reynolds number, $L\rho_e V_e/\mu_{01}$
Re_S Reynolds number, $S\rho_e V_e/\mu_{01}$
Re^{**} Reynolds number, $\delta^{**}\rho_e V_e/\mu_{01}$
Re_h^{**} Reynolds number, $\delta_h^{**}\rho_e V_e/\mu_{01}$
S channel width
St Stanton number, $q_w/\rho_e V_e(h_w - h_{re}^*)$
T temperature
t time
V velocity
x longitudinal coordinate
y coordinate normal to the wall.

Greek symbols

α heat transfer coefficient
δ boundary layer thickness
$\bar{\delta}^{**}$ dimensionless momentum thickness, δ^{**}/δ
$\bar{\delta}_h^{**}$ dimensionless energy loss thickness, δ_h^{**}/δ
θ dimensionless enthalpy, $(h^* - h_w)/(h_e^* - h_w)$
λ thermal conductivity
ξ dimensionless coordinate, y/δ
ρ density
$\bar{\rho}$ dimensionless density, ρ/ρ_e
τ friction stress
$\bar{\tau}$ dimensionless friction stress, τ/τ_w
ω dimensionless velocity, V_x/V_e.

Subscripts

e boundary layer edge
f mean-mass temperature
h thermal boundary layer
in value at $t = 0$
inj injection
w wall
0 standard boundary layer
01 channel entrance
1,2 channel wall.

$$P = \rho RT = \frac{K-1}{K}\rho\left(h^* - \frac{V_x^2}{2}\right). \quad (7)$$

After simple transformations, the system of equations (1)–(7) gives the integral momentum, continuity and energy equations.

2.1. *A channel with plane or annular cross-section*

The system of integral equations for the initial section of the channel is formulated for the first wall in the form of a momentum equation

$$\frac{L}{V_e}\frac{\partial}{\partial t}(H'_1 Re_1^{**}) + \frac{\partial Re_1^{**}}{\partial \bar{x}} - \left[\frac{I_1 Re_L}{H_{31}^\gamma V_e} + \frac{L Re_1^{**}(H'_1 - H_1)}{V_e^2}\right]\frac{\partial V_e}{\partial t} + \frac{1}{V_e}\left[Re_1^{**}(H_1 + 1) - \frac{I_1 Re_L}{L H_{31}^\gamma}\right]\frac{\partial V_e}{\partial \bar{x}} + \frac{Re_1^{**}}{H_{31}^\gamma}\frac{\partial H_{31}^\gamma}{\partial \bar{x}} - \frac{I_1 Re_L}{L\rho_e V_e^2 H_{31}^\gamma}\frac{\partial P}{\partial \bar{x}} = \left(b_{w1} + \frac{C_{f1}}{2}\right) Re_L \quad (8)$$

and an energy equation

$$\frac{\partial}{\partial t}\left(\frac{H'_{h1} H_{31}^\gamma L\, Re_{h1}^{**}\Delta h_1}{V_e}\right) + \frac{I_1 Re_L}{\rho_e V_e}\frac{\partial P}{\partial t} - \frac{L}{V_e}\left[H_{31}^\gamma\, Re_1^{**}(H_1 - H_1) + \frac{I_1 Re_L}{L}\right]\frac{\partial h_e^*}{\partial t} + H_{31}^\gamma \Delta h_1 \frac{\partial Re_{h1}^{**}}{\partial \bar{x}} + \left(Re_{h1}^{**} H_{31}^\gamma + H_1\, Re_1^{**} H_{31}^\gamma - \frac{I_1 Re_L}{L}\right)\frac{\partial h_e^*}{\partial \bar{x}} - H_{31}^\gamma\, Re_{h1}^{**}\frac{\partial h_{w1}}{\partial \bar{x}} + \Delta h_1\, Re^{**}\frac{\partial H_{31}^\gamma}{\partial \bar{x}} = (b_{w1} + St_1)\Delta h_{11} H_{31}^\gamma\, Re_L; \quad (9)$$

for the second wall in the form of a momentum equation

$$\frac{L}{V_e}\frac{\partial}{\partial t}(H'_2\, Re_2^{**}) + \frac{\partial Re_2^{**}}{\partial \bar{x}} - \left[\frac{I_2\, Re_L}{H_{32}^{\gamma} V_2^2} + \frac{L\, Re_2^{**}(H'_2 - H_2)}{V_e^2}\right]\frac{\partial V_e}{\partial t} + \frac{1}{V_e}\left[Re_2^{**}(H_2+1) - \frac{I_2\, Re_L}{LH_{32}^{\gamma}}\right]\frac{\partial V_e}{\partial \bar{x}} + \frac{Re_2^{**}}{H_{32}^{\gamma}}\frac{\partial H_{32}^{\gamma}}{\partial \bar{x}} - \frac{I_2\, Re_L}{L\rho_e V_e^2 H_{32}^{\gamma}}\frac{\partial P}{\partial \bar{x}} = \left(b_{w2} + \frac{C_{f2}}{2}\right) Re_L \qquad (10)$$

an energy equation

$$\frac{\partial}{\partial t}\left(\frac{H'_{h2} H_{32}^{\gamma} L\, Re_{h2}^{**}\, \Delta h_2}{V_e}\right) + \frac{I_2\, Re_L}{\rho_e V_e}\frac{\partial P}{\partial t} - \frac{L}{V_e}\left[H_{32}^{\gamma}\, Re_2^{**}(H'_2 - H_2) + \frac{I_2\, Re_L}{L}\right]\frac{\partial h_e^*}{\partial t} + H_{32}^{\gamma}\Delta h_2 \frac{\partial Re_{h2}^{**}}{\partial \bar{x}} + \left(Re_{h2}^{**}\, H_{32}^{\gamma} + H_2\, Re_2^{**}\, H_{32}^{\gamma} - \frac{I_2\, Re_L}{L}\right)\frac{\partial h_e^*}{\partial \bar{x}} - H_{32}^{\gamma}\, Re_{h2}^{**}\frac{\partial h_{w2}}{\partial \bar{x}} + \Delta h_2\, Re_{h2}^{**}\frac{\partial H_{32}^{\gamma}}{\partial \bar{x}} = (b_{w2} + St_2)\Delta h_{12} H_{32}^{\gamma}\, Re_L \qquad (11)$$

and a continuity equation

$$\frac{\partial}{\partial t}\left[\frac{L\, Re_1^{**}\, H_{31}^{\gamma}(H'_1 - H_1)}{V_e} + \frac{L\, Re_2^{**}\, H_{32}^{\gamma}(H'_2 - H_2)}{V_e} + \frac{I_3\, Re_L}{V_e}\right] - H_1 H_{31}^{\gamma}\frac{\partial Re_1^{**}}{\partial \bar{x}} - H_2 H_{32}^{\gamma}\frac{\partial Re_2^{**}}{\partial \bar{x}} + \frac{I_3\, Re_L}{L}\left(\frac{1}{V_e} + \frac{V_e}{h_e}\right)\frac{\partial V_e}{\partial \bar{x}} + \frac{I_3\, Re_L}{LP}\frac{\partial P}{\partial \bar{x}} - \frac{I_3\, Re_L}{Lh_e}\frac{\partial h_e}{\partial \bar{x}} + \frac{Re_L}{L}\frac{\partial I_3}{\partial \bar{x}} - H_{31}^{\gamma}\, Re_1^{**}\frac{\partial H_1}{\partial \bar{x}} - H_{32}^{\gamma}\, Re_2^{**}\frac{\partial H_2}{\partial \bar{x}} - H_1\, Re_1^{**}\frac{\partial H_{31}^{\gamma}}{\partial \bar{x}} - H_2\, Re_2^{**}\frac{\partial H_{32}}{\partial \bar{x}} - \frac{I_3\, Re_L}{LK(K-1)}\frac{\partial K}{\partial \bar{x}} = (H_{31}^{\gamma} b_{w1} + H_{32}^{\gamma} b_{w2})\, Re_L. \qquad (12)$$

For the channel section after the convergence of the boundary layers, equations (8), (10), and (12) retain their forms. Equation (3) is reduced to

$$\frac{\partial}{\partial t}\left(\frac{H'_{h1} H_{31}^{\gamma}\, Re_{h1}^{**} L\, \Delta h_1}{V_e}\right) + \frac{\partial}{\partial t}\left(\frac{H'_{h2} H_{32}^{\gamma}\, Re_{h2}^{**} L\, \Delta h_2}{V_e}\right) + \frac{I_3\, Re_L}{\rho_e V_e}\frac{\partial P}{\partial t} - \left[H_{31}^{\gamma}\, Re_1^{**}(H'_1 - H_1) + H_{32}^{\gamma}\, Re_2^{**}(H'_2 - H_2) + \frac{I_3\, Re_L}{L}\right]\frac{L}{V_e}\frac{\partial h_e^*}{\partial t} + H_{31}^{\gamma}\Delta h_1 \frac{\partial Re_{h1}^{**}}{\partial \bar{x}} + H_{32}^{\gamma}\Delta h_2 \frac{\partial Re_{h2}^{**}}{\partial \bar{x}} + \left(Re_{h1}\, H_{31}^{\gamma} + H_1\, Re_1^{**}\, H_{31}^{\gamma} + Re_{h2}^{**}\, H_{32}^{\gamma} + H_2\, Re_2^{**}\, H_{32}^{\gamma} - \frac{I_3\, Re_L}{L}\right)\frac{\partial h_e^*}{\partial \bar{x}} + H_{31}^{\gamma}\, Re_{h1}^{**}\frac{\partial h_{w1}}{\partial \bar{x}} + H_{32}^{\gamma}\, Re_{h2}^{**}\frac{\partial h_{w2}}{\partial \bar{x}} - Re_{h1}^{**}\Delta h_1 \frac{\partial H_{31}}{\partial \bar{x}} - Re_{h2}^{**}\Delta h_2 \frac{\partial H_{32}^{\gamma}}{\partial \bar{x}} = (b_{w1} + St_1)\Delta h_{11}\, Re_L\, H_{31}^{\gamma} + (b_{w2} + St_2)\Delta h_{12}\, Re_L\, H_{32}^{\gamma}. \qquad (13)$$

Since the region of inviscid flow is absent, equations (5) and (6) are replaced by the following geometric relations:

$$\delta_1 = \delta_{h1}; \quad \delta_2 = \delta_{h2} \qquad (14)$$

$$\delta_1 + \delta_2 = S \qquad (15)$$

which are transformed to

$$-\frac{1}{\tilde{\delta}_1^{**}}\frac{\partial Re_1^{**}}{\partial \bar{x}} + \frac{1}{\tilde{\delta}_{h1}^{**}}\frac{\partial Re_{h1}^{**}}{\partial \bar{x}} = \frac{Re_{h1}^{**}}{\tilde{\delta}_{h1}^{**}}\frac{\partial \tilde{\delta}_{h1}^{**}}{\partial \bar{x}} - \frac{Re_1^{**}}{\tilde{\delta}^{**2}}\frac{\partial \tilde{\delta}_1^{**}}{\partial \bar{x}} \qquad (16)$$

$$-\frac{1}{\tilde{\delta}_2^{**}}\frac{\partial Re_2^{**}}{\partial \bar{x}} + \frac{1}{\tilde{\delta}_{h2}^{**}}\frac{\partial Re_{h2}^{**}}{\partial \bar{x}} = \frac{Re_{h2}^{**}}{\tilde{\delta}_{h2}^{**2}}\frac{\partial \tilde{\delta}_{h2}^{**}}{\partial \bar{x}} - \frac{Re_2^{**}}{\tilde{\delta}_2^{**2}}\frac{\partial \tilde{\delta}_2^{**}}{\partial \bar{x}} \qquad (17)$$

$$\frac{1}{\tilde{\delta}_1^{**}}\frac{\partial Re_1^{**}}{\partial \bar{x}} + \frac{1}{\tilde{\delta}_2^{**}}\frac{\partial Re_2^{**}}{\partial \bar{x}} - Re_S\left(\frac{1}{V_e} + \frac{V_e}{h_e}\right)\frac{\partial V_e}{\partial \bar{x}} - \frac{Re_S}{P}\frac{\partial P}{\partial \bar{x}} + \frac{Re_S}{h_e}\frac{\partial h_e^*}{\partial \bar{x}} = \frac{Re_1^{**}}{\tilde{\delta}_1^{**2}}\frac{\partial \tilde{\delta}_1^{**}}{\partial \bar{x}} + \frac{Re_2^{**}}{\tilde{\delta}_2^{**2}}\frac{\partial \tilde{\delta}_2^{**}}{\partial \bar{x}} + \frac{Re_S}{S}\frac{\partial S}{\partial \bar{x}} - \frac{Re_S}{K(K-1)}\frac{\partial K}{\partial \bar{x}}.$$

Here, the following notations were adopted:

$$\delta^* = \int_0^{\delta}(1-\tilde{\rho}\omega)\left(1 \pm \frac{y}{R_w}\cos\beta\right)dy;$$

$$\delta^{**} = \int_0^{\delta}\tilde{\rho}\omega(1-\omega)\left(1 \pm \frac{y}{R_w}\cos\beta\right)dy;$$

$$\delta^{*\prime} = \int_0^{\delta}\tilde{\rho}(1-\omega)\left(1 \pm \frac{y}{R_w}\cos\beta\right)dy;$$

$$\delta_h^{**} = \int_0^{\delta}\tilde{\rho}\omega(1-\theta)\left(1 \pm \frac{y}{R_w}\cos\beta\right)dy;$$

$$\delta_h^{**'} = \int_0^{\delta} \tilde{\rho}(1-\theta)\left(1 \pm \frac{y}{R_w}\cos\beta\right) dy.$$

2.2. *A circular channel*

The system of integral equations is formulated as follows:

momentum equation

$$\frac{L}{V_e}\frac{\partial}{\partial t}(H'\,Re^{**}) - \frac{1}{V_e^2}\left[L\,Re^{**}(H'-H) + Re_L\,\delta\left(1-\frac{\delta}{2R_w}\right)\right]\frac{\partial V_e}{\partial t} + \frac{\partial Re^{**}}{\partial \bar{x}} + \frac{1}{V_e}\left[Re^{**}(H+1) - \frac{Re_L\,\delta}{L}\left(1-\frac{\delta}{2Re_w}\right)\right] \times \frac{\partial V_e}{\partial \bar{x}} - \frac{Re_L\,\delta}{L\rho_e V_e^2}\left(1-\frac{\delta}{2R_w}\right)\frac{\partial P}{\partial \bar{x}} + \frac{Re^{**}}{R_w}\frac{\partial R_w}{\partial \bar{x}} = \left(b_w + \frac{C_f}{2}\right)Re_L; \quad (18)$$

energy equation

$$\frac{\partial}{\partial t}\left(\frac{H_h'\Delta h L\,Re_h^{**}}{V_e}\right) - \frac{L}{V_e}\left[Re^{**}(H'-H) + \frac{Re_L\,\delta}{L}\left(1-\frac{\delta}{2R_w}\right)\right]\frac{\partial h_e^*}{\partial t} + \Delta h\frac{\partial Re_h^{**}}{\partial \bar{x}} + \left[Re_h^{**} + H\,Re^{**} - \frac{Re_L\,\delta}{L}\left(1-\frac{\delta}{2R_w}\right)\right] \times \frac{\partial h_e^*}{\partial \bar{x}} - Re_h^{**}\frac{\partial h_w}{\partial \bar{x}} + \frac{\Delta h\,Re_h^{**}}{R_w}\frac{\partial R_w}{\partial \bar{x}} + \frac{Re_L\,\delta}{\rho_e V_e}\left(1-\frac{\delta}{2R_w}\right)\frac{\partial P}{\partial t} = (b_w + St)\Delta h_1\,Re_L; \quad (19)$$

continuity equation

$$\frac{\partial}{\partial t}\left[\frac{L\,Re^{**}(H'-H)}{V_e} + \frac{Re_L\,R_w}{2V_e}\right] - H\frac{\partial Re^{**}}{\partial \bar{x}} + \frac{Re_L\,R_w}{2L}\left(\frac{1}{V_e}+\frac{V_e}{h_e}\right)\frac{\partial V_e}{\partial \bar{x}} + \frac{Re_L\,R_w}{2LP}\frac{\partial P}{\partial \bar{x}} - \frac{Re_L\,R_w}{2Lh_e}\frac{\partial h_e^*}{\partial \bar{x}} - Re^{**}\frac{\partial H}{\partial \bar{x}} - \frac{Re_L\,R_w}{K(K-1)L}\frac{\partial K}{\partial \bar{x}} - \left(\frac{H\,Re^{**}}{R_w} - Re_L\right)\frac{\partial R_w}{\partial \bar{x}} = b_w\,Re_L. \quad (20)$$

For the initial section equations (18)–(20) are supplemented with equations (5) and (6). Over the length after the convergence of the boundary layers equations (5) and (6) are substituted by the following geometric conditions:

$$\delta = R_w; \quad \delta_h = R_w \quad (21)$$

which are reduced to the form

$$\frac{1}{\tilde{\delta}^{**}}\frac{\partial Re^{**}}{\partial \bar{x}} - Re_R\left(\frac{1}{V_e}+\frac{V_e}{h_e}\right)\frac{\partial V_e}{\partial \bar{x}} - \frac{Re_R}{P}\frac{\partial P}{\partial \bar{x}} + \frac{Re_R}{h_e}\frac{\partial h_e^*}{\partial \bar{x}} = \frac{Re^{**}}{\tilde{\delta}^{**2}}\frac{\partial \tilde{\delta}^{**}}{\partial \bar{x}} + \frac{Re_L}{L}\frac{\partial R_w}{\partial \bar{x}} - \frac{Re_R}{K(K-1)}\frac{\partial K}{\partial \bar{x}} \quad (22)$$

$$\frac{1}{\tilde{\delta}_h^{**}}\frac{\partial Re_h^{**}}{\partial \bar{x}} - Re_R\left(\frac{1}{V_e}+\frac{V_e}{h_e}\right)\frac{\partial V_e}{\partial \bar{x}} - \frac{Re_R}{P}\frac{\partial P}{\partial \bar{x}} + \frac{Re_R}{h_e}\frac{\partial h_e^*}{\partial \bar{x}} = \frac{Re_h^{**}}{\tilde{\delta}_h^{**2}}\frac{\partial \tilde{\delta}_h^{**}}{\partial \bar{x}} + \frac{Re_L}{L}\frac{\partial R_w}{\partial \bar{x}} - \frac{Re_R}{K(K-1)}\frac{\partial K}{\partial \bar{x}}. \quad (23)$$

Here

$$Re_R = \frac{R_w\rho_e V_e}{\mu_{01}}.$$

2.3. *Relative laws of friction and heat transfer*

Integration of the system of momentum, continuity and energy equations becomes possible after the establishment of the relationship between the friction, C_f, and heat transfer, St, coefficients and correspondingly between the Reynolds numbers, Re^{**} and Re_h^{**}. Moreover, the determination of the integral characteristics H, H', and H_h' requires the knowledge of the velocity, ω, and enthalpy, θ, profiles. Following ref. [3], the coefficients C_f and St will be represented as

$$C_f = \Psi C_{f0} \quad (24)$$

$$St = \Psi_h\,St_0. \quad (25)$$

The relative laws of friction Ψ and heat transfer Ψ_h in equations (24) and (25) contain all the information about the difference of the studied boundary layer with disturbing factors (non-isothermicity, pressure gradient, permeability, etc.) from the 'standard' boundary layer for which

$$C_{f0} = 2(2.5\ln Re^{**} + 3.8)^{-2} \quad (26)$$

$$St_0 = (2.5\ln Re_h^{**} + 3.8)^{-2}\,Pr^{-0.75}. \quad (27)$$

A system of equations will now be derived for the unsteady turbulent flow with regard, in the general case, for non-isothermicity, permeability, compressibility and adverse pressure gradient. Representing the flow shear in Prandtl's form, it is possible to write

$$\tau = \rho l^2\left(\frac{\partial V_x}{\partial y}\right)\left|\frac{\partial V_x}{\partial y}\right| \quad (28)$$

$$q = -\frac{\lambda_T}{C_p}\left(\frac{\partial h^*}{\partial y}\right). \quad (29)$$

The characteristic turbulence scale l in equation (28) is defined as

$$l = \kappa y \sqrt{\tilde{\tau}_0}. \tag{30}$$

It follows from equations (28) and (30) that

$$\tilde{\tau} = \tilde{\rho}\kappa^2 \xi^2 \tilde{\tau}_0 \frac{2}{C_f}\left(\frac{\partial \omega}{\partial \xi}\right)^2. \tag{31}$$

Integrating equation (31) over the boundary layer thickness, the dimensionless velocity profile can be determined

$$\omega = \frac{1}{\kappa}\sqrt{\left(\frac{C_{f0}}{2}\Psi\right)}\int_0^{\xi}\sqrt{\left(\frac{1}{\tilde{\rho}}\frac{\tilde{\tau}}{\tilde{\tau}_0}\right)}\frac{d\xi}{\xi}. \tag{32}$$

Taking into account that $\xi = 1$ when $\omega = 1$, the relative friction law can be obtained from equation (32)

$$\Psi = \left(\frac{1}{\frac{1}{\kappa}\int_0^1 \sqrt{\left(\frac{1}{\tilde{\rho}}\frac{\tilde{\tau}}{\tilde{\tau}_0}\right)}\frac{d\xi}{\xi}}\right)^2 \frac{2}{C_{f0}}. \tag{33}$$

Equations (28) and (29) can yield

$$\frac{q}{\tau} Pr_T \frac{\partial \omega}{\partial \xi}\frac{V_e}{\delta} = \frac{(h_w - h_e^*)}{\delta}\frac{\partial \theta}{\partial \xi}. \tag{34}$$

Integration of equation (34) over the boundary layer thickness gives the dimensionless enthalpy profile

$$\theta = \frac{\Psi_h}{\Psi} Pr_T\left(\frac{\tilde{q}}{\tilde{\tau}} - \int_0^{\xi}\omega\frac{d(\tilde{q}/\tilde{\tau})}{d\xi}d\xi\right)\frac{\Delta h_1}{\Delta h}\frac{C_{f0}}{2St_0}. \tag{35}$$

With the use of the conditions $\xi = 1$ and $\theta = 1$ on the edge of the boundary layer, equation (35) gives the relative law of heat transfer

$$\Psi_h = \frac{\Psi}{Pr_T\left(1 - \int_0^1 \omega\frac{d(\tilde{q}/\tilde{\tau})}{d\xi}d\xi\right)}\frac{\Delta h}{\Delta h_1}\frac{2St_0}{C_{f0}}. \tag{36}$$

The density distribution in equations (32) and (33) is determined from the relation

$$\frac{1}{\tilde{\rho}} = \psi - \Delta\psi\theta - (\psi^* - 1)\omega^2 \tag{37}$$

where

$$\psi = \frac{h_w}{h_e}; \quad \psi^* = \frac{h_e^*}{h_e}; \quad \Delta\psi = \psi - \psi^*.$$

The distribution of flow shear and heat flux density over the boundary layer thickness is approximated by the relations which were suggested in ref. [4] and which have the following form for the conditions considered:

$$\frac{\tilde{\tau}}{\tilde{\tau}_0} = \exp\left[\tilde{\tau}'_w \xi(1-\xi)\right] \tag{38}$$

$$\frac{\tilde{q}}{\tilde{q}_0} = \exp\left[\tilde{q}'_w \xi(1-\xi)\right]. \tag{39}$$

Equations (38) and (39) can yield

$$\frac{\tilde{q}}{\tilde{\tau}} = \exp\left[(\tilde{q}'_w - \tilde{\tau}'_w)\xi(1-\xi)\right]. \tag{40}$$

Here

$$\tilde{\tau}'_w = \left.\frac{d\tilde{\tau}}{d\xi}\right|_w; \quad \tilde{q}'_w = \left.\frac{d\tilde{q}}{d\xi}\right|_w. \tag{41}$$

As is seen from the above relations, the distributions of $\tilde{\tau}$ and $\tilde{q}$ depend on the magnitude and sign of the quantities $\tilde{\tau}'_w$ and $\tilde{q}'_w$, the governing equations for which are derived as follows. For the conditions on the wall equations (2) and (3) give

$$(\rho V_y)_w \left.\frac{\partial V_x}{\partial y}\right|_w = -\frac{\partial P}{\partial x} + \left.\frac{\partial \tau}{\partial y}\right|_w \pm \frac{\tau_w}{R_w} \tag{42}$$

$$\rho\frac{\partial h_w^*}{\partial t} + (\rho V_y)_w \left.\frac{\partial h^*}{\partial y}\right|_w = \frac{\partial P}{\partial t} - \left.\frac{\partial q}{\partial y}\right|_w \pm \frac{q_w}{R_w}. \tag{43}$$

Whence, with equations (5) and (6) taken into account

$$\tilde{\tau}'_w = \Lambda + Re_{inj} \pm \frac{\delta}{R_w} \tag{44}$$

$$\tilde{q}'_w = z_h + Re_{inj}\, Pr \pm \frac{\delta}{R_w}. \tag{45}$$

Here

$$\Lambda = \frac{2\delta}{C_f \rho_e V_e^2}\frac{\partial P}{\partial x} \tag{46}$$

where Λ is the parameter of the longitudinal pressure gradient, $Re_{inj} = (\rho V_y)_w \delta/\mu_w$ the Reynolds number based on the permeability parameters

$$z_h = \frac{\delta}{St\,\rho_e V_e (h_w - h_{re}^*)}\left(\frac{\partial P}{\partial t} - \rho_w \frac{\partial h_w}{\partial t}\right)$$

the parameter of the thermal unsteady state.

3. DISCUSSION OF RESULTS

The closed systems of equations obtained, which describe the unsteady heat transfer and friction of a turbulent gas flow in a channel of plane, annular or circular cross-section, were realized as a FORTRAN program for an EC electronic computer. The accuracy of the mathematical model and its numerical realization were estimated by comparing the predicted and experimental data obtained by different authors. Some of the results of this comparison are given below. The calculated results for the hydrodynamics and heat transfer parameters of an isothermal air flow in a tube are presented in Figs. 1–4. The flow in the initial section of the tube is often compared with the flow on a plate. In fact, the dynamic and thermal boundary layers start to develop downstream from the tube entrance and, in the first approximation, the calculation of friction and heat transfer can be made

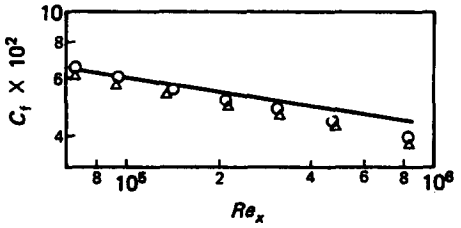

FIG. 1. Friction factor over the initial tube section: ——, prediction; ○, $C_f = 0.576Re_x^{-0.2}$; △, $C_f = 0.592Re_x^{-0.2}$.

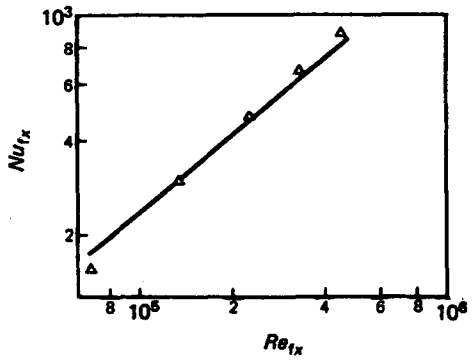

FIG. 3. Heat transfer over the initial section of the tube: ——, prediction; △, $Nu_{fx} = 0.021Re_{fx}^{0.8}\,Pr_f^{0.43}\,(x/d)^{0.2}(Pr_f/Pr_w)^{0.25}$.

by relations obtained for a plate. However, there is also one distinctive feature—the presence of the adverse pressure gradient. Velocity in the flow core does not remain constant due to the thickening of the boundary layers. The behaviour of the maximum velocity on the tube axis along its length with respect to the velocity at the tube is depicted in Fig. 4. The velocity on the axis increases to about 1.3 of the inlet velocity and then remains constant. It was shown in ref. [5] that at the instant of the convergence of dynamic boundary layers the maximum velocity should comprise about 1.24 of the inlet value. According to the estimates [5, 6], the hydrodynamic length amounts to about $18S$–$20S$. As is seen from Fig. 4, the predicted length of the initial section is equal to $22S$ which is close to that obtained experimentally. It should be noted that in the initial section of the tube there is actually the zone of laminar flow the length of which depends on the Reynolds number $Re_d = V_f S_{eq}/\nu_f$ at the inlet [6]. Due to the flow acceleration, the friction factor in the initial section of the tube is higher than that for the plate [2]. It is seen from Fig. 1 that the predicted value of C_f is higher than that obtained experimentally in refs. [2, 5]. As to the heat transfer coefficient, a weaker effect of flow acceleration on it can be noted. In Fig. 2 the predicted and experimental values of the heat transfer coefficients are given, with the temperature on the axis being taken as dominating. It can be noted that the predicted values lie somewhat above the experimental data of ref. [2]. On the other hand, these very prediction results, processed using the mean-mass temperature (Fig. 3), lie below those given by the well-known Mikheyev equation [7].

The thermal initial section for gases is somewhat shorter than the dynamic one. The information about its length is very inconsistent, but, as the authors of ref. [2] deduce from the generalization of many works, this value is close to $15S$. In ref. [6] this value is given to be equal to $20S$–$30S$. It should be noted here that the length of the thermal initial section depends strongly on the flow conditions. Calculations made for a small non-isothermicity factor give the initial thermal length to be equal to about $16S$ in conformity with the data of ref. [2].

Figures 5 and 6 present the results of calculations for a plane channel. The behaviour of the friction factor C_f in Fig. 5 is the same as in the tube inlet section, with the plot for a plate being located somewhat below. The predicted heat transfer coefficient (Fig. 6) coincides with that obtained experimentally in ref. [2]. The same calculated results but processed with the aid of Mikheyev's equation (Fig. 7) are somewhat overstated.

The computed results processed on the basis of the equivalent diameter $Nu_d = \alpha d_{eq}/\lambda$ are given in Fig. 8. Also presented are the experimental data of refs. [8, 9]. It is seen that the length of the initial thermal section is equal to about $20S$. The coincidence between the predicted and experimental values can be considered satisfactory.

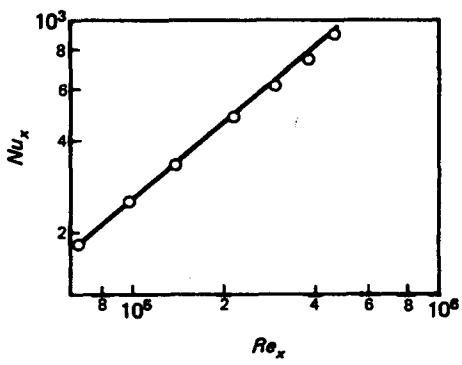

FIG. 2. Heat transfer over the initial section of the tube: ——, prediction; ○, $Nu_x = 0.0289Re^{0.8}\,Pr^{0.4}$.

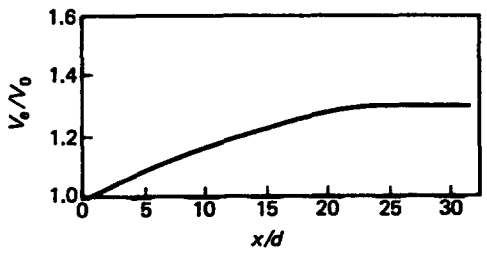

FIG. 4. Variation of the maximum velocity along the tube length.

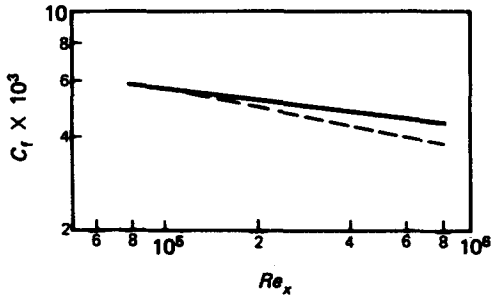

FIG. 5. Friction in the inlet section of a plane channel: ——, prediction; – – – –, $C_f = 0.576 Re_x^{-0.2}$.

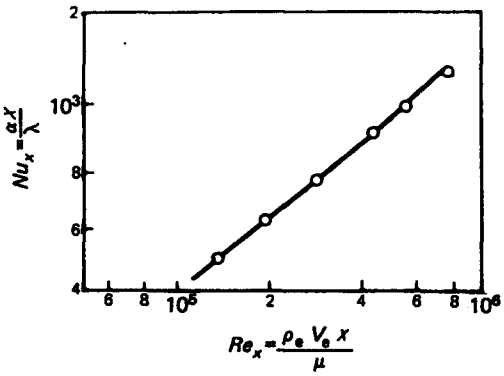

FIG. 6. Heat transfer in the inlet section of a plane channel: ——, prediction; ○, $Nu_x = 0.0128 Re_x^{0.83} Pr^{0.4}$.

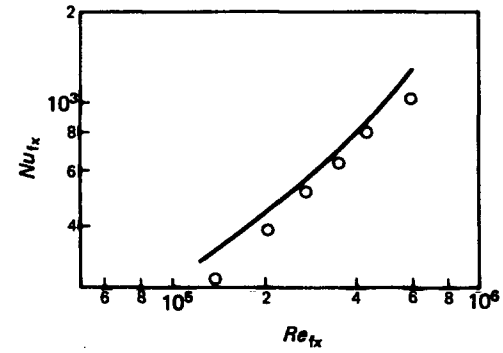

FIG. 7. Heat transfer in the inlet of a plane channel: ——, prediction; ○, $Nu_{fx} = 0.021 Re_{fx}^{0.8} Pr_f^{0.43} (x/d)^{0.2} (Pr_f/Pr_w)^{0.25}$.

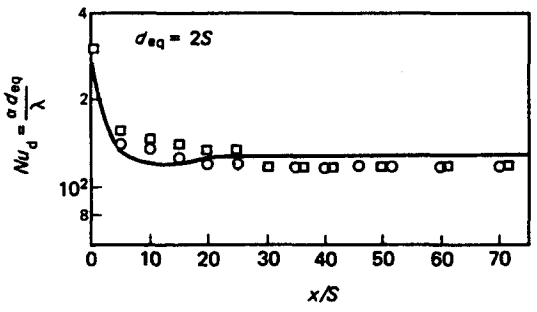

FIG. 8. Heat transfer in a plane channel: ——, prediction; +, ref. [8]; ○, ref. [9].

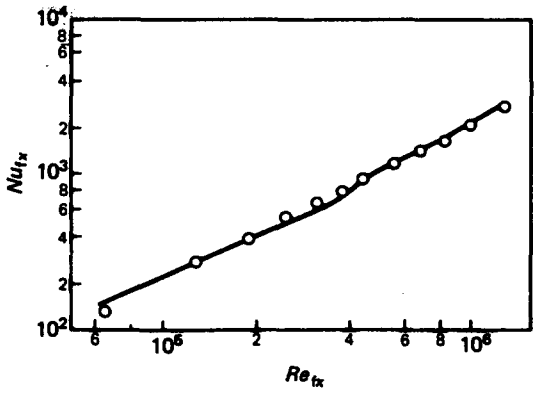

FIG. 9. Heat transfer in a plane channel: ——, prediction; ○, $Nu_{fx} = 0.21 Re_{fx}^{0.8} Pr_f^{0.43} (x/d)^{0.2} (Pr_f/Pr_w)^{0.25}$.

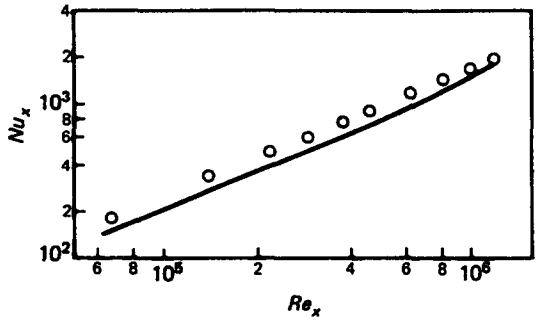

FIG. 10. Heat transfer in a plane channel: ——, prediction; ○, $Nu_x = 0.0218 Re_x^{0.83} Pr^{0.4}$.

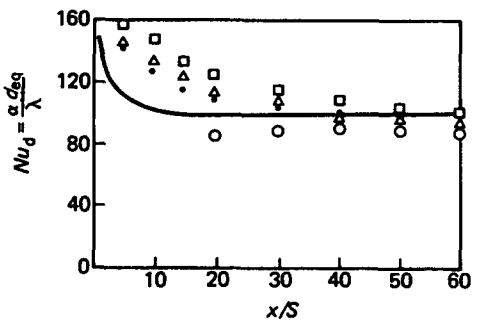

FIG. 11. Heat transfer in a plane channel: ——, prediction; △, +, ○, refs. [2, 5, 6].

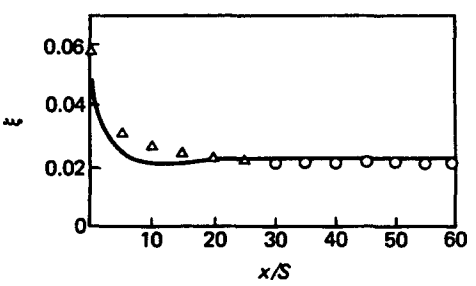

FIG. 12. Resistance coefficient in a plane channel: ——, prediction; △, ref. [2]; ○, refs. [5, 6].

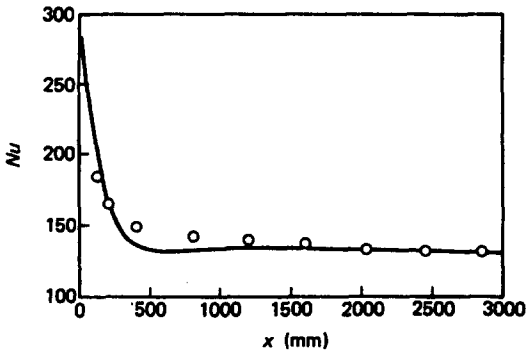

FIG. 13. Heat transfer on the inner wall of an annular channel in the case of asymmetric heat transfer: ——, prediction; O, ref. [11].

Figures 9–12 present the results of calculations of heat transfer and friction in a plane channel at substantial non-isothermicity factors ($\geqslant 2$). In Fig. 9 the results of calculations are processed by the mean-mass flow temperature and include both the initial section and the section after the convergence of the boundary layers. The computational relation almost coincides with Mikheyev's equation [7]. In Fig. 10, the results of calculations are compared with the data of ref. [2]. Over the initial section the latter data lie somewhat higher than the former, but become closer after the convergence of the boundary layers. It should be noted here that the experimental relation was obtained by the authors of ref. [2] only for the entry section and it does not include the effect of the non-isothermicity factor on the heat transfer coefficient. At the same time, the relation suggested in ref. [7], with which the comparison is made in Fig. 9, takes into account the effect of the temperature factor. Figure 11 presents the results of calculations processed by the equivalent diameter and the experimental data of refs. [5, 8–10]. It should be noted that the experimental data of refs. [8–10] were mainly obtained for the section after the convergence of the boundary layers and, moreover, for the case of gas cooling, with correcting factors being introduced for the inlet section. Figure 12 shows the behaviour of the resistance factor ξ along the channel length. For the initial section, the experimental data of ref. [2] for a tube converted into the equivalent diameter are given for comparison and for the section after the convergence of the boundary layers the experimental data of refs. [5, 6] are presented also converted into the equivalent diameter. In the initial section the deviation of the predicted relations from those obtained experimentally is observed. However, the authors of ref. [6] indicate that when extending the results of the experiments carried out under non-isothermal flow conditions to the isothermal case, it is necessary to introduce correction in the form of the non-isothermicity factor raised to a certain power. In ref. [2] such a correction was not made and this explains the discrepancy between the computed and experimental data. The comparison of the results of calculation of asymmetric heat transfer in an annular channel with the experimental data of ref. [11] is given in Fig. 13. As is seen from the comparative analysis of the predicted and experimental data, the developed mathematical model adequately describes the turbulent heat transfer and friction in gas flows through channels of different cross-sections.

REFERENCES

1. G. A. Dreitser and P. M. Markovskiy, Generalization of experimental data on unsteady-state heat transfer in the case of the heated gas flow rate variation in a round tube under the turbulent flow conditions, *Gidravlika* No. 6, 106–112 (1977).
2. A. S. Sukomel, V. I. Velichko and Yu. G. Abrasimov, *Heat Transfer and Friction in Turbulent Flow of Gases Through Short Channels*. Izd. Energiya, Moscow (1979).
3. S. S. Kutateladze and A. I. Leontiev, *Heat Transfer and Friction in a Turbulent Boundary Layer*. Energoatomizdat, Moscow (1985).
4. N. Tetervin, Approximate calculation of Reynolds analogy for turbulent boundary layer with pressure gradient, *AIAA J.* No. 6, 1079–1085 (1969).
5. A. I. Leontiev (Editor), *Heat Transfer Theory*. Izd. Vysshaya Shkola, Moscow (1979).
6. E. K. Kalinin, G. A. Dreitser, V. V. Kostyuk and I. I. Berlin, *Methods of Calculation of Conjugated Heat Transfer Problems*. Izd. Mashinostroyeniye, Moscow (1983).
7. M. A. Mikheyev (Editor), *Mean Heat Transfer in Fluid Motion Through Tubes*. Izd. AN SSSR, Moscow (1959).
8. G. A. Dreitser, E. K. Kalinin and V. A. Kuzminov, Unsteady-state convective heat transfer with different laws of hot gas cooling in tubes, *J. Engng Phys.* **25**(2), 208–216 (1973).
9. N. I. Artamonov, Yu. I. Danilov, G. A. Dreitser and E. K. Kalinin, Experimental investigation of local heat transfer and hydraulic resistance of a gas cooled in tubes, *Teplofiz. Vysok. Temp.* **8**(6), 1228–1234 (1970).
10. G. A. Dreitser, V. D. Evdokimov and E. K. Kalinin, Unsteady-state convective heat transfer of a fluid heated in a tube by a variable heat flux, *J. Engng Phys.* **31**(1), 5–12 (1976).
11. B. S. Petukhov and L. I. Roizen, Experimental investigation of heat transfer in turbulent flow of gas in tubes of annular cross-section, *Teplofiz. Vysok. Temp.* **1**(3), 19–24 (1963).

TRANSFERT THERMIQUE ET FROTTEMENT POUR UN ECOULEMENT TURBULENT DE GAZ DANS DES CANAUX AVEC DIFFERENTES SECTIONS DROITES

Résumé—On considère des écoulements de gaz dans des canaux avec sections droites circulaires, annulaires ou rectangulaires. Un modèle mathématique est proposé qui utilise une approche intégrale pour décrire les transferts de quantité de mouvement et d'énergie dans une couche limite turbulente. On suppose que les couches limites dynamiques et thermiques se développment simultanément sur les parois du canal pour converger.

WÄRMEÜBERGANG UND DRUCKABFALL IN EINER TURBULENTEN GASSTRÖMUNG IN KANÄLEN VON UNTERSCHIEDLICHER QUERSCHNITTSFORM

Zusammenfassung—Die Gasströmung in Kanälen von kreisförmigem, kreisringförmigem und rechteckigem Querschnitt wird betrachtet. Es wird ein mathematisches Modell vorgeschlagen, in dem für die Beschreibung des Impuls- und Energietransports in einer turbulenten Grenzschicht ein Integralansatz verwendet wird. Es wird angenommen, daß sich die hydrodynamische und die thermische Grenzschicht an der Kanalwand gleichzeitig zu entwickeln beginnen und nach und nach zusammenwachsen.

ТЕПЛООБМЕН И ТРЕНИЕ ПРИ ТУРБУЛЕНТНОМ ТЕЧЕНИИ ГАЗА В КАНАЛАХ РАЗЛИЧНОГО СЕЧЕНИЯ

Аннотация—Рассматривается течение газа в каналах круглого кольцевого и плоского сечения. Предлагаемая математическая модель использует интегральный подход для описания процессов переноса импульсов и энергии в турбулентном пограничном слое. Предполагается, что динамический и тепловой пограничные слои начинают нарастать на стенках канала одновременно и в дальнейшем смыкаются.